Proceedings World Geothermal Congress 2020+1
Reykjavik, Iceland, April - October 2021

1D Inversion of Magnetotelluric Data From Ashute, Butajira Geothermal Prospect, South-East Ethiopia And Its Geothermal Implications

Tsegaye Wondifra Tadesse

josywondifra@gmail.com

Keywords: Ashute, Butajira, Geothermal, Magnetotelluric (MT) and 1D inversion model

ABSTRACT

All Geophysical surveying is one of the Earth Science disciplines which is used for exploration of geothermal energy. A magnetotelluric (MT) survey was conducted in the Ashute Geothermal prospect area acquiring 28 soundings. The major objectives of the study were to define the assumed upflow zone of the geothermal fluid. North-South of the major hydrothermal manifestations in the Ashute field and to make the suggest cross-section maps and 1D inversion model, to study the subsurface resistivity structure of the geothermal system at the Ashute, Butajira field, generally, low resistivity in the area is the result of the thick lacustrine sediment deposits with in intercalated with pyroclastic ash flow in Ashute field. its relation to the geothermal field marked Aligned volcanic cones and the group of thermal spring in the axial part of Debre zait Selti graven suggest the main NE – SW Debre zait Selti fault system and transverse NW – SE older rift structure beyond to control Magmatism (heat source), water recharge and permeability of the system. Two possible heat source are thought to be associated with young basaltic eruptions and intrusions < 0.13 Ma, and silicic centers identified in the southern part of the area. The project area is covered by pyroclastic ash flow and volcanic sediment, mapped as a single unit. Within it we have pyroclastic ash flow deposits and graded sediment deposits ranging from ash to gravel sized. The flat, lowland of the Butajira and Ashute plain is covered by these pyroclastic and sediment deposits, deposited at the same geologic time, and stratigraphically they are set together one on another in undefined pattern.

Of the MT survey maps a low conductivity zone (less than 10 Ωm) in the North-South Ashute field, thought to delineate the up-flow zone of the geothermal fluid, and circulation of the geothermal fluid is deduced to be related to the structure; all thermal springs in the area are found along a single fault - the Southward extension of Ajira –Afuno normal fault. We have identified two separate structural patterns from aerial photographs and from the resistivity cross sections and interpretation maps. The trend of high and low resistivity anomalies, the discontinuous structure (NE-SW alignment) and transverse NW-SE faults and opening fissures, indicate the possibility of the connection of the Ashute and the Butajira geothermal systems. In addition to this survey, more MT soundings are recommended towards the NE-SW Ashute geothermal field and BTJ-068 in the Ashute field, and a reinterpretation of result using TEM data for a better definition of the anomalies, and thus achieve the stated exploration objectives.

1. INTRODUCTION

Exploration for geothermal resources in Ethiopia close to the rift margin has been carried out since 1970s. The different regional exploration activities concern both national and international organizations. Geological surveys have been done for the whole rift at a scale of one to half a million. Geological, geochemical and airborne geophysical results have identified 16 geothermal prospect areas in the rift. Later additional explorations were conducted and currently the prospect areas are around 24, and the estimated potential > 10,000 MWe. The Butajira Selti prospect area is on the western fault border of the rift axis. Previously, geothermal exploration was focused on the axis and the eastern part of the active fault system of the Main Ethiopia Rift (MER) particularly on the Wonji fault system in both southern and northern Afar rift. The project area was recommended in United Nation Development Programme (UNDP) technical report (1973) for further detailed geological and geochemical study. The area was regarded as a low enthalpy geothermal resource which can be used for direct use rather than electrical generation. Then in April 2014 a sudden explosion of hot thermal fluid occurred during deep drilling of an irrigation well. This potentially hazardous situation changed previous thoughts and required detailed exploration work.

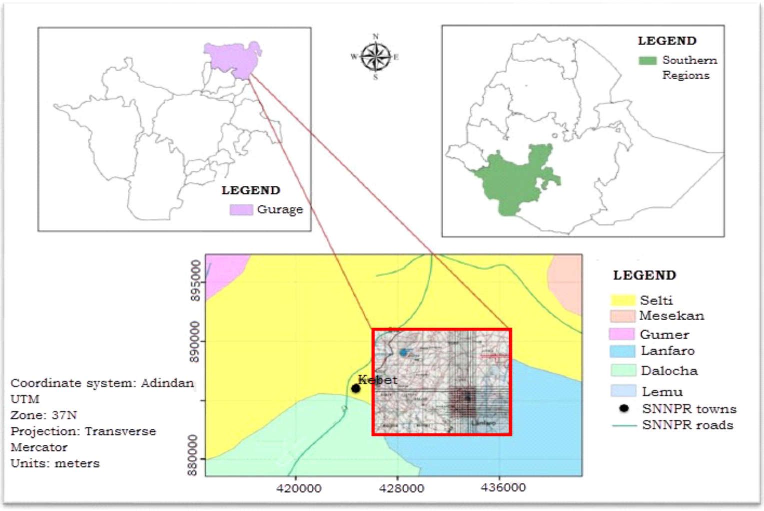

Figure 1: Location and accessibility of The Project Area (Gebrewold, 2017)

The Ashute, Butajira geothermal field is located in the Southern Nations Nationalities Regional State, the south-western part of the Western margin of the Main Ethiopian Rift, about 150 km southeast of Addis Ababa in the low plain of Ethiopian Rift (Figure 1). The nearby towns are Butajira and Kebet in Selti Wereda. The prospect area lies within two zones of the state administration namely Gurage and Selti zone. It is bound by (8° 08' 32.9" N to 7° 51' 42.8" N and 38° 13' 10.7" E to 38° 32' 13.9653" E. The highway from Addis Ababa to Hosanna in the west vicinity of Garage high land runs in northeast direction in the low plain of rift valley. There is gravel road from Kebet Selti Wereda to the Ashute prospect area. The weather is dry and the road is unpaved.

2. THE GEOLOGY OF THE STUDY AREA

The Main Ethiopian Rift (MER) is the northern part of the East African Rift System (EARS) where opportunites to study the difference in volcanism (mainly composition and volumes) as a function of the extension along the rift margin. As stated by Abebe et al., 2007, and Pizzi et al., 2006 the erupted material along MER can be divided into two different compositions. The northern most part is mostly characterized by basaltic lava flows, connected with a flat area of volcanoes and erupted fissures (e.g. Hayward and Ebinger, 1996; Lahitte et al., 2003). In contrast, the central and southern part of the rift are the home to felsic central volcanoes, typical characterized by calderas, iable for the released of rhyolite and ignimbrites (e.g. Woldegabriel et al., 1990; Chernet et al., 1998; Ebinger and Casey, 2001; Acocella et al., 2003). These accumulations of volcanic materials are usually interlaid with sedimentary rift deposits (Le Turdu et al., 1999). According to Mohr (1962) the general Quaternary volcano-tectonic setting of the MER is described as an overlapping spreading center where the Wonji Fault Belt (WFB) is the eastern limb. These NNE-SSW Quaternary rift zones of the WFB form areas of active deformation of a fault that has both horizontal and vertical elements of displacement of the rift floor of the MER (Figure 2).

Both silicic and basaltic rocks are found in the study area (Figure 3). The compositional variation in the rock units is due to volcanism in the MER and is described by a two peaked basalt-rhyolite group (Abebe et al., 2007). The lithological units are scoria (defining lithology for a volcanic centre (scoria cones) in the study area), highly vesicular basalt, igneous rock containing abundant vesicles, layered pumice, pyroclastic flow deposits with a strong variation in textural features (porphyritic to a pyritic type). Table 1 lists the rock units in the area. The rocks are strongly weathered overlain with soil as thick as 0.5 meter. Crystalline ignimbrite (containing xenolith of basalt and rhyolite) and lacustrine sediment deposits (lake deposits of sandstone and conglomerate) are also observed.

2.1. The general geological and tectonic settings of the Ethiopia Rift System

The MER is an approximately NE trending sector of the East African Rift system that contains a series of rift segments that increase in size from the Afar Triple Junction (at the Red Sea-Gulf of Aden intersection) to the Kenya Rift. The MER is characterised by active oblique extensional tectonics, with a spreading rate of 6–7 mm/yr. It has an extension strain involving an increase in length of more than 5,000 km from the Red Sea up to Mozambique through the East African Rift System, where most of the great African lakes are located (Marco et al., 2005)

As determined by to many authors (e.g. Bonini, 2005; Mohr, 1983; Woldegabriel et al., 1990; Hayward and Ebinger, 1996), the MER has been divided into three segments: (1) the Southern (2) the Central and (3) the Northern MER. These three segments symbolize distinct stages of the extension processes, from early rifting in the Southern MER to the more develop gradually stages in the Central and Northern MER the spreading has started to develop into normal seafloor spreading as the Afar (Hayward and Ebinger, 1996).

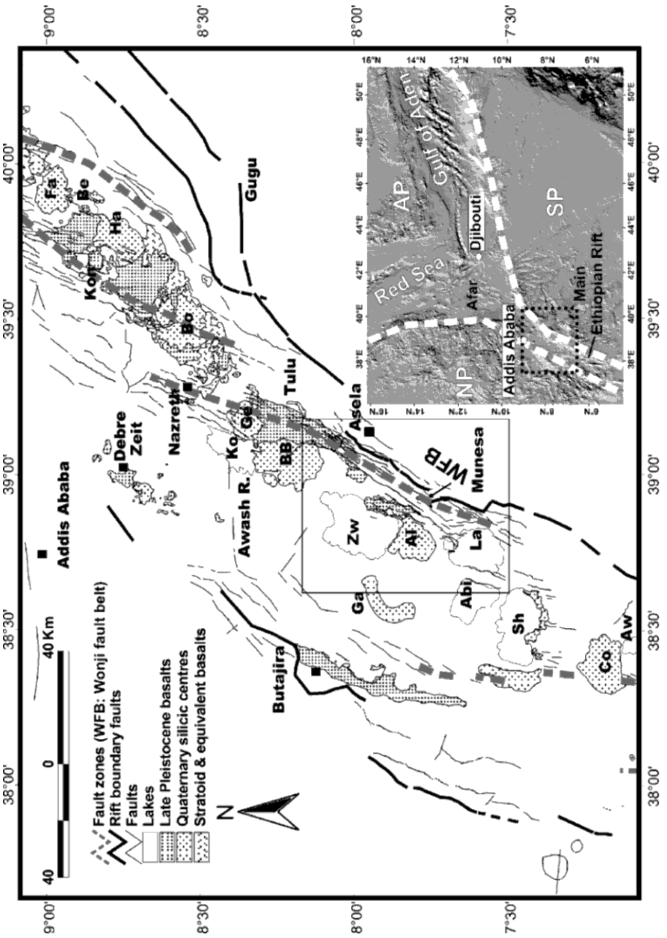

Figure 2: Structural map of the northern sector of the Main Ethiopian Rift (MER) with major faults. The study area is within the rectangle. Trend of fault zones includes the WFB which in the study area constitutes the eastern side of the MER Lakes. The inset map shows the plate tectonics of the Afar triple junction. Artificially shaded topographic and bathymetric data SRTM 30 with the light coming from the NW with a 608 inclination. Dashed rectangle shows location of the geological map on Figure 3. Lakes:Aw, Awasa; Sh,Shala; Abi,Abijata; La,Langano; Zw,Zway; Ko,Koka; Be,Beseka. *Volcanoes: Co,Corbetti; Ga, Gademota; Al, Aluto; BB, Bora Bericcio, Ge, Gedemsa; Bo, Bosetti; Ha, Hada; Kon,Kone; Fa, Fantale.* NP, Nubian plate;SP, Somalian plate; AP, Arabian plate. (Pizzi et al., 2006).

3. OBJECTIVES OF THE STUDY AREA

The main objectives of the proposed geophysical studies are:

- Process MT data from the Ashute prospect and do 1D inversion of the data. Present the resulting model as resistivity cross-sections and depth slices for geothermal interpretation.

- To pursue the resistivity anomaly mapped in Ashute in the general NE-SW direction with the transverse faults in the different orientation and find the depth to the geothermal reservoir.

- To identify the subsurface resistivity distribution of the area and detect the characterization of a possible geothermal system and locate drilling targets.

3.1 Geothermal Exploration

Geothermal exploration in Ethiopia has a long history the estimated potential of geothermal resources is more than 10,000 MW. So far only a very little fraction of the total potential is harnessed. In order to avert possible shortfalls and also due to their added advantage in complementing the hydro generation during unfavorable periods of severe droughts, geothermal development in Ethiopia has been given more attention in recent years (Kebede, 2014).

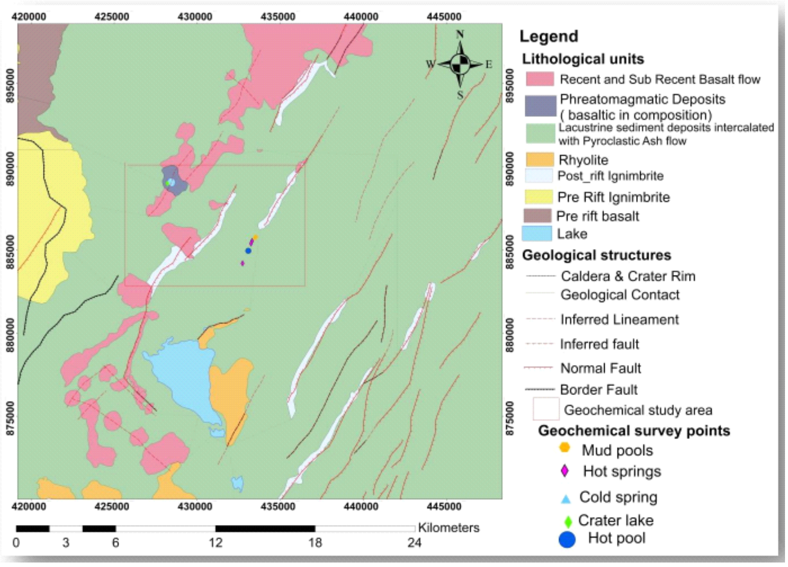

Figure 3: Geological map of the study area (modified from Abebe et al., 2017)

3.2 Resistivity of rocks

Geothermal water interacts with rocks which undergo a chemical and physical change secondary mineralization depending on the different temperature and pressure. Resistivity depends on the type of alteration, temperature and salinity of the fluid. The distribution of alteration minerals provides information on the temperature of the geothermal system, the flow path of geothermal water and the physicochemical characteristics of the geothermal water. At temperatures from 100°C to 220°C, low-temperature zeolites and smectite clay mineral are formed (Árnason et al., 2000). Smectite could be hydrated and loosely bound cations between the silica plates make the mineral conductive with high cation exchange capacity (CEC). Therefore, a conductive zone is formed where low-temperature zeolites and smectites are abundant, which is called the smectite-zeolite zone. In the temperature range from 220°C to about 250°C, the low-temperature zeolites disappear and the smectite changes to chlorite in a transition zone, called the mixed-layer clay zone, where smectite and chlorite coexist in a mixture. At about 250°C the smectite disappears and chlorite becomes the dominant alteration mineral. At still higher temperatures, about 240 – 250°C, epidote becomes abundant in the chlorite-epidote zone. This zoning is relevant for fresh water basaltic systems. The up doming conductive smectite layer often indicates up flow of the system with corresponding outflows to its side away from the up flow. It also happens that alteration minerals show a sign of lower temperature than measured in the wells. This has been interpreted as being due to a young system being heated up and the alteration is lagging behind, still not in equilibrium with the temperature (Hersir and Árnason, 2009).

4. MT INSTRUMENTATION, DATA ACQUISITION AND PROCESSING

4.1 Instrumentaion , data acquisition and processing

The MT survey in Butajira, Ashute field was conducted along 8 EW profiles (Figure 4). They stretch over the geothermal surface manifestation area and are oriented nearly perpendicular to the general regional structural trend, the NE-SW direction. The profile and station intervals are about 1 km and 1.5 km, respectively while in Ashute the profiles are laid out as infill profiles close to the surface manifestations.

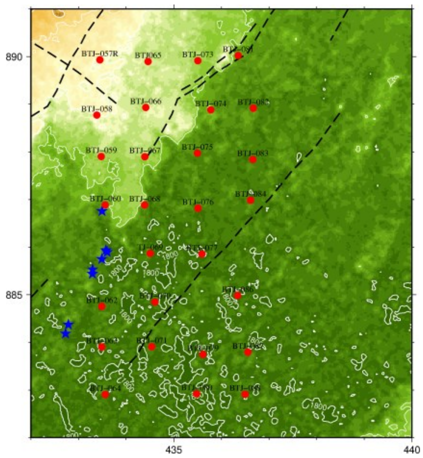

Figure 4: Location of the MT stations (red dots). Blue stars are geothermal surface manifestations and the black dash lines are faults

On each survey day, two MT measurements were done and the time series of the amplitudes of the five components of the EM field (E_x, E_y, H_x, H_y and H_z) were recorded by the data logger at the center. The time series data were recorded for about 21 hours between 10 A.M and 7 A.M. The electro-magnetic fields were in the frequency range between 320 H_z and 0.001 H_Z. From this frequency range, MT parameters at more than 50 frequencies were calculated.

4.2 Data quality evaluation and processing and time series

Data processing and interpretation generally involve two stages as indicated in Figure 5. The processing steps in the flow chart were mostly carried out using the software SSMT2000, Synchro time series viewer, MTEditor, from Phoenix Geophysics.

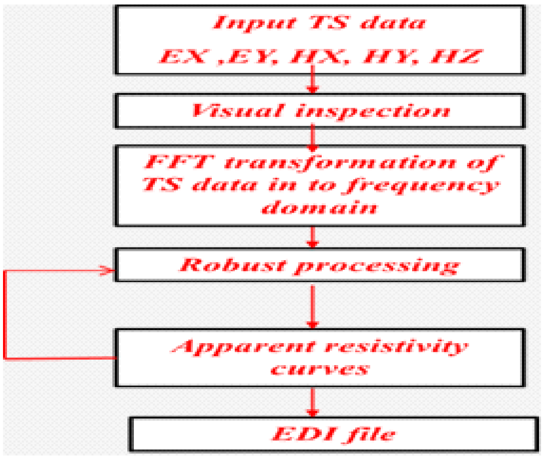

Figure 7: Flow chart: (from MT phoenix geophysics user guide)

Figure 5: MT processing flow chart: (from MT phoenix geophysics user guide)

Data Processing involves various actions on the data. First the data from the compact flash is down loaded onto a laptop computer. Visual inspection of the recorded data on site and a preliminary time series processing in the field camp were done on a daily basis to ensure acceptable data quality for later processing and interpretation. This is followed by transformation of the time series data from time domain to frequency domain. The processing is a multiple coherency based stacking of spectra, is a routine statistical method which derives estimates of MT impedance tensor elements MT response functions that are relatively smooth unbiased by outliers, was done in SSMT2000 (Phoenix Geophysics, 2005). With reference to these parameters on the display, cross-power data consisting of 40 segments were edited for noise to reduce the standard deviation and enhance resistivity continuity and when data quality ensured (example shown in Figure 6).

4.3 1D inversion of MT data using the TEMTD Program

The TEMTD program can perform 1D inversion for both TEM and MT data, separately or jointly (Árnason, 2006). TEMTD solves both the forward and inverse problems. The inversion problem is to find those model parameters which give a model response close to the measured data. The forward problem calculates the response from given model parameters. The programme gives the possibility of keeping the model smooth with respect to resistivity variations between layers.

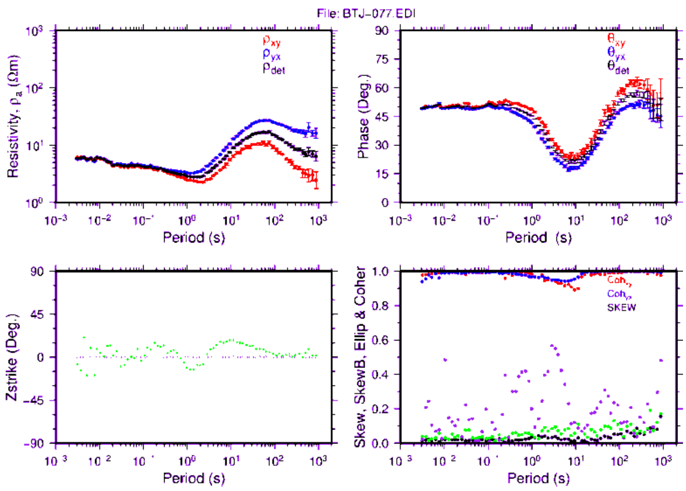

Figure 6: An example of MT processed data (station BTJ-077) from the prospect area. Processed data from all the MT soundings are in Appendix I in the Appendices report (Tadesse, 2018). The apparent resistivity and phase for different parameters:, and which is derived from the determinant of the impedance are shown on the figure as well as the Zstrike, skew, ellipticity and coherency.

5. RESULTS OF MT RESISTIVITY MODELING AND THE INTERPRETATION FROM ASHUTE GEOTHERMAL FIELD

Interpretation of the MT data is the second stage in the data processing and interpretation sequence. Firstly, it is necessary to check the static shift in the data. Then the data are analyzed and inverted to yield the electrical resistivity structure of the Earth below the recording station and its variation both laterally and vertically. The directionality and dimensionality of the impedance tensors and their changes with frequency (depth) are evaluated and determined. A 1D inversion is perfomred and the resistivity model integrated with other geodata. In this project area, 1D resistivity models were obtained and inversion later production of maps and cross-sections produced in Linux. Data from the EDI files for each MT station, output from MTEditor, were inverted using the TEMTD program (Árnason, 2006) . Occam inversion was used and the input was the rotationally invariant apparent resistivity and phase calculated from the determinant of the impedance tensor (see e.g. Lemma, 2010). In the project area 28 MT stations on 11 profiles were used in the 1D inversions for this project (Figure 4).

5.1 1D inversion modelling of MT data from Ashute

The apparent resistivity and phase were inverted for assuming a smoothed 1D Earth model. The resistivity varies only with depth and hence, the MT impedance tensor is independent of the orientation of the measurement axes. Target zones are relatively low resistivity zones that could be associated with conductive pyroclastic ash flow deposit, sediments and hydrothermally altered zones, showing significant areal distribution and thickness within a relatively shallow depth range. These might be underlain by zones of relatively high resistivity that could be correlated with high temperature alteration zones possibly the core of high temperature geothermal reservoir. Resistivity discontinuities might serve as structures for the circulation of geothermal fluid. Figure 7 shows an example of 1D Occam inversion of MT data. Marked and also it show the values of chi and shift, on the other right side it shows the resistivity model with at different depth.

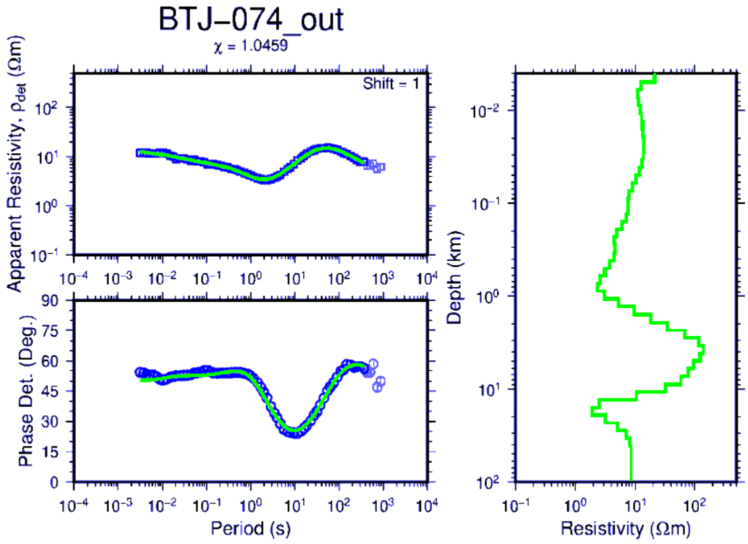

Figure 7: 1D Occam inversion of MT sounding BTJ-074. Blue squares are the apparent resistivity and blue circles the phase, both calculated from the determinant value of the impedance. The light blue symbols to the right of the green curve are data points not used in the inversion, the green curves on the panels to the left show the MT apparent resistivity and phase responses from the resistivity model to the right. The number on top of the figure (BTJ-074) is the name of the sounding while χ is the misfit function.

The 1D models provide information on the resistivity structure of the subsurface versus depth. The models are often presented as resistivity cross-sections and depth slices. Zones of low resistivity values at shallow depths are often the cap rock of the geothermal reservoir. The underlying relatively higher resistivity zone, the resistive core, is sometimes associated with high temperature hydrothermal alteration zone while resistivity discontinuities might serve as conduits to circulation of geothermal fluid.

The conductive zone in Ashute delineates a zone marked by 10 Ωm and less. It is observed to have a general NE-SW orientation that extends from the surface to a maximum depth of about 450 m. The zone is flanked to the northeast and southwest by slightly higher resistivity. In the southwestern portion the Ashute hot springs and hydrothermally altered zone coincide with a slightly high resistivity zone.

In general, the marginal Debre zait Selti rift graben suggests a main NE – SW Debre zait Selti fault system and transverse NW – SE older rift structure which is controlled by magmatism (heat source), water recharge and permeability of the system. Two possible heat sources are expected these are directly associated with the young basaltic eruptions and intrusion < 0.13 Ma and silicic centers located in the southern part of the area. Possible enrichment of these units by shallow/deep geothermal fluid is expected to enhance the conductivity as can be witnessed from a very low resistivity values observed on these maps.

The influence of the NE-SW and NNE structures are better seen on the low resistivity contours at Ashute on most of the maps. That might reflect its association with high permeability around the intersection of faults/fractures with varying orientation. A trace of ENE structure could be inferred at Ashute area and the observed central low resistivity contours seen on most of the maps is still opened towards the south east.

5.2 The resistivity cross-sections from Ashute

Resistivity cross-sections were produces using TEMCROSS programme developed at ISOR (Eysteinsson, 1998) along the eight resistivity profiles parallel to the general tectonic structure; profile 1, 2, 3, 4, 5, 6, 7, 8, 9, 10 and 11 based on the 1D layered resistivity models as shown in Appendix II in the Appendices report (Tadesse, 2018). The locations of the MT soundings are shown on Figure 4. The cross-sections along profile 1 and profile 3 are discussed below.

The cross-sections along profiles 1 and 3 are shown in Figure 8, down to a depth of 5,000 m b.s.l. The cross-sections generally display three resistivity layers in the Ashute field. The first layer is marked by medium low resistivity values, less than 30 Ωm. It is observed to stretch across some of the profiles with varying thicknesses. On profile 1 and profile 3 from MT sounding BTJ-067 and further to the east, the layer is 1,800 m thick and reaches down to a depth of 200 m a.s.l. The Ashute area is characterized by a conductive shallow lying layer with an average thickness of about 1,800 m in general. The cross-sections are relatively similar and the prospect area is flat. The subsurface is composed of the volcanic sediments including lithified ash, fine to coarse sandstone, well laminated conglomerate and debris or lahar. The clasts mostly consist of pyroclastic material derived from silicic center from the south. They can be correlated to sediments at shallow depth and the low resistivity of resistivity less than 10 Ωm. Following the low resistivity zone there is high resistivity and a 3rd zone of even higher resistivity. The 1D models provide information on the resistivity structure of the subsurface versus depth. The models are often presented as resistivity cross-sections and depth slices. Zones of low resistivity values at shallow depths are often the cap rock of the geothermal reservoir. The underlying relatively higher resistivity zone, the resistive core, is sometimes associated with high temperature hydrothermal alteration zone while resistivity discontinuities might serve as conduits to circulation of geothermal fluid.

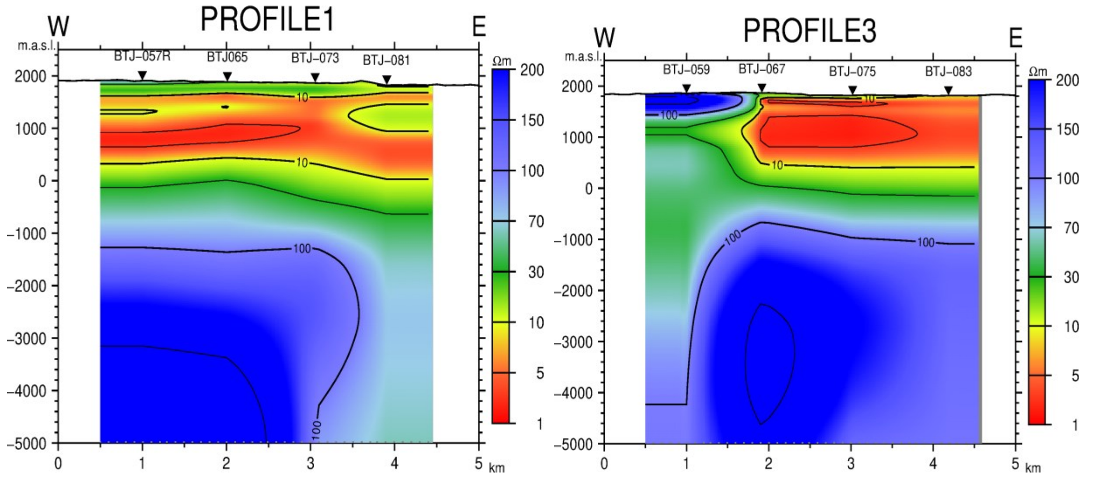

Figure 8: Resistivity cross-sections along profiles 1 and 3 (same colour scale). MT locations s in Figure 4.

The conductive zone in Ashute delineates a zone marked by 10 Ωm and less. It is observed to have a general NE-SW orientation that extends from the surface to a maximum depth of about 450 m. The zone is flanked to the northeast and southwest by slightly higher resistivity. In the southwestern portion the Ashute hot springs and hydrothermally altered zone coincide with a slightly high resistivity zone.

In general, the marginal Debre zait Selti rift graben suggests that the main NE – SW Debre zait Selti fault system and transverse NW – SE older rift structure control magmatism (heat source), water recharge and permeability of the system. Two possible heat sources are expected these are directly associated with the young basaltic eruptions and intrusion < 0.13 Ma and silicic centers located in the southern part of the area. Possible enrichment of these units by shallow/deep geothermal fluid is expected to enhance the conductivity as can be witnessed from a very low resistivity values observed on these maps.

The influence of the NE-SW and NNE structures are better seen on the low resistivity contours at Ashute on most of the maps. That might reflect its association with high permeability around the intersection of faults/fractures with varying orientation. A trace of ENE structure could be inferred at Ashute area and the observed central low resistivity contours seen on most of the maps is still opened towards the southeast greater than 70 Ωm which is probably related to fractured basalt and scoria.

The uppermost conductive layer on the cross section along profile 3 indicates a structure between station BTJ-059 and BTJ-067. The low resistivity layer on the cross section along profile 3 is nearly uniform in thickness, around 1400 m reaching down to a depth of some 600 m. This layer is not seen below MT station BTJ-059.

The MT method assumes that the earth structure is one-dimensional that there is a dip and strike. Therefore, most MT stations are acquired along profiles 1D or on a grid 2-D from which profiles can be extracted. Almost all MT interpretation is done in 1-D inversion, usually dip lines. There are 2-D codes available, but they still require large amounts of computing power and are not normally practical for prospect-level exploration problems. The MT interpreter takes the processed data and interprets it to a representation of true resistivity versus depth. This can be done using forward or inverse modeling. With forward modeling, the interpreter creates a cross-section, computes the MT response and compares it with the acquired data; for inverse modeling, the interpreter allows the computer to create a cross-section from the acquired data. Both types of modeling result in cross-sections or maps of the subsurface where the resistivity of the subsurface is interpreted to represent certain geologic formations or units.

5.3 Resistivity depth slices from Ashute

Resistivity depth slices were produced using the TEMRESD programme developed at ISOR (Eysteinsson, 1998) to plot horizontal resistivity maps based on the 1D layered resistivity models as. Two depth slices are discussed below, 1,000 m a.s.l and 500 m b.s.l (Figure 9).

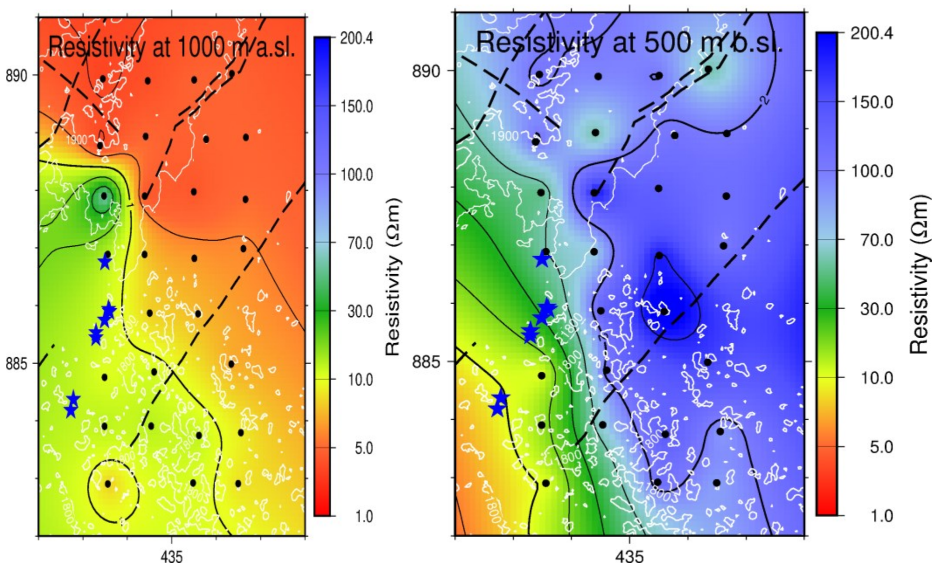

Figure 9: Resistivity depth slices at 1000 and 500 m b.s.l. Same colour scale in both. The blue stars are geothermal surface manifestations, the black dash lines are faults and the black dots are MT soundings.

Resistivity depth slice at 1,000 m a.s.l.: In general the map displays very low resistivity between 1 Ωm and 5 Ωm in the north and northeast part of the survey area. A relatively high resistivity greater than 70 Ωm is observed in the southwest section of the area. The discontinuity in the Debre zait Selti graben suggests that the main NE – SW Debre zait Selti fault system and transverse NW – SE older rift structure control the magmatism (heat source), water recharge and permeability of the system. The overall low resistivity in the area is an attribute of the thick lacustrine sediment deposits intercalated with pyroclastic ash flow in the Ashute field. The high resistivity seen on the shallow maps around Ashute signifies that the recent and sub recent basalt flow, phreatomagmatic deposits and volcanic crater lake in which basalt is intensively weathered from bottom to top of the crater. The high resistivity mapped around Ashute could be a response to the recent and sub recent basalt flow.

Resistivity map at 500 m b.s.l.: The high resistivity in the northeast part of the survey area, greater than 70 Ωm, is probably because of lithological variations due to recent and sub recent basalt flow and phreatomagmatic deposits. The resistivity structure is oblique to the NW – SE old rift structure.

6. STRIKE ANALYSIS

Zstrike is determined through a horizontal rotation that maximizes the off-diagonal elements of the MT impedance tensor and minimizes the diagonal elements using the sum of the squared modulus of these elements. Zstrike has 90º ambiguity and the strike direction can't be determined from the MT impedance alone. This ambiguity is resolved using a parameter that doesn't depend on the impedance tensor elements, known as Tipper vector provided that H_z is measured at the measurement site (Vozoff, 1991). The generalization of dimensionality is also made using the Tipper magnitude of the magnetotelluric transfer function. The magnitude of the Tipper depends on the presence of lateral conductivity variations. Low Tipper magnitude or very close to zero is related to 1D resistivity structures while high Tipper magnitude imply, generally, non 1D conductivity structure.

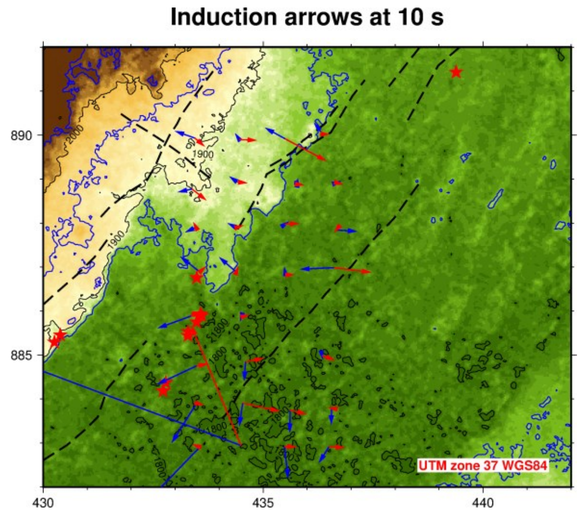

Figure 10: Induction arrows at 10 s. Red arrows are imaginary part and blue arrows the real part. Red stars are geothermal surface manifestations and the black dash lines are the faults.

Strike analyses have been performed in this work by producing maps showing induction arrows at 10 s (Figure 10), rose diagram of the Tipper strike for 0.5 - 1 s (Figure 11) and rose diagram of the Zstrike for 0.1 - 0.5 s (Figure 12). These maps are discussed below.

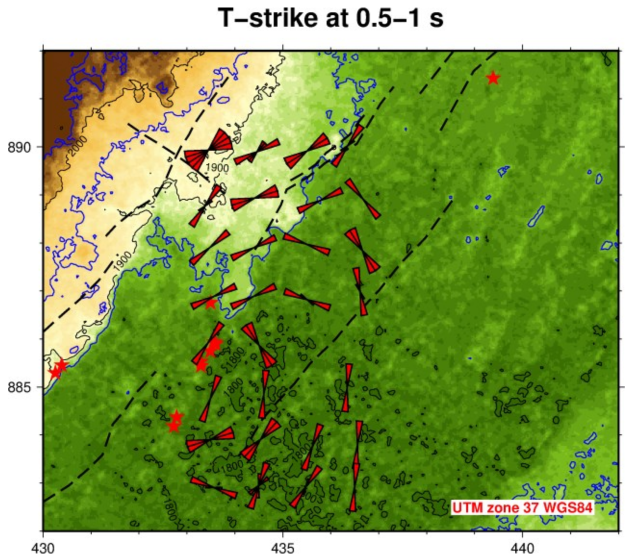

Figure 11: Rose diagram showing the Tipper strike at 0.5-1 s. Red stars are geothermal surface manifestations and the black dash lines are the faults

The Zstrike for 0.1-0.5 s (Figure 12) shows the geoelectrical strike direction at shallow depths (high frequency) and reflects the dominant NE-SW geological strike direction of the area, note the change of the strike direction in the NW corner of the Figure. The Tipper strike on Figure 11 is shown for lower frequency reflecting greater depth. Here, most likely a significant change in the geological strike direction is observed. Figure 17 shows the induction arrows at very low frequency or great depths. The arrows are small indicating small resistivity contrasts at these depths as seen on the resistivity cross-sections above.

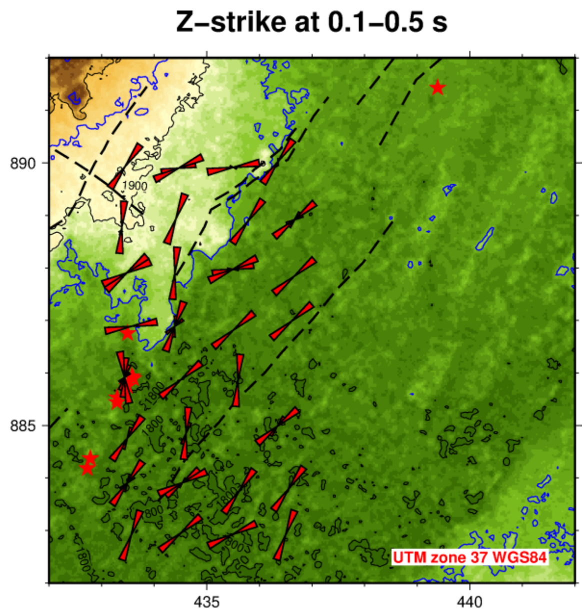

Figure 12: Rose diagram showing the Zstrike at 0.1-0.5 s. Red stars are geothermal surface manifestations and the black dash lines are the faults

7. CONCLUSION

The sporadic nature of the orientation of the resistivity contour lines for different depth levels suggests that the Ashute field is structurally complex, as indicated by the presence of the different orientations of the faults and fractures in the area. In this project some 28 MT soundings have been processed and 1D inverted. The results are presented as resistivity cross sections and depth slices and compared to the geological findings.

The Ashute area is characterized by a conductive shallow lying layer with resistivity values less than 10 Ωm and an average thickness of about 1,800 m in general. It reaches down to a depth of 200 m a.s.l. The subsurface is composed of the volcanic sediments including lithified ash, fine to coarse sandstone, well laminated conglomerate and debris or lahar. The clasts mostly consist of pyroclastic material derived from silicic center from the south. They can be correlated to sediments at shallow depth and the low resistivity. Below the low resistivity there is high resistivity with resistivity greater than 70 Ωm which is probably related to the basement, fractured basalt and scoria.

The high resistivity below the conductive zone likely reflects the influence of major fault systems, the tectonic trend of the Debre zait Selti rift graben and the Main Ethiopian Rift (MER).

Geothermal fluid at depth emerges to shallow level most likely along the NE-SW discontinuity and NW-SE structures, flowing laterally and enriching the shallow permeable formation and appearing as thermal manifestations in the field.

The strike analyses for different depth levels (frequencies) indicate a general NE-SW strike direction for shallow depths which coincides with the major trend of the western rift axis. At greater depths the geo-electrical structure changes.

8. RECOMMENDATIONS

In this project area there are no TEM soundings. Therefore, it is recommended to do TEM at the same location as the MT sites to correct for the static shift of the MT data. Thereafter, to jointly invert the TEM and MT data before taking any drilling action around the suggested promising sites from this study. It is furthermore recommended to add MT and co-located TEM soundings towards the north and west of the Ashute field to better define the resistivity structures. Detailed geological mapping of the area, in particular the tectonics are recommended, and gravity surveying to delineate geological structures.

REFERENCES

Abebe, T., Alemu, T., 2007: Geology and Tectonic evaluations of the Pan- African Tulu Dimtu Belt, Western Ethiopia. *Journal of Earth Sciences* 1 (1): 24 – 42.

Abebe, T., Mazarini, F., Innocenti, F., Manneti, P., 1998: The Yerer-Tulu wellel volcano-tectonic lineament, atransitional structure in central Ethiopia, and the associated magmatic activity. *J. Afr. Earth Sci.* 26 (1), 135-150.

Abebe, Z., Sinetebeb, Y., Eshetu, A., 2017: Surface geothermal exploration mapping of Butajira- Selti area Ethiopia. *Geological survey of Ethiopia (GSE*), Unpublished report 1, 28 pp.

Acocella, V., Korme, T., Salvini, F., 2003: Formation of normal faults along the axial zone of the Ethiopian rift. *J. Struct. Geol*. 25, 503–513.

Árnason K., 2006: TEMTD, A Programme for 1D inversion of central-loop TEM and MT data. *Short manual. ISOR, Iceland Geosurvey*. Unpublished, 17 pp.

Árnason, K., Karlsdóttir, R., Eysteinsson, H., Flóvenz, Ó.G., and Gudlaugsson, S.Th., 2000: The resistivity structure of high-temperature geothermal systems in Iceland. *Proceedings of the World Geothermal Congress 2000*, Kyushu-Tohoku, Japan, 923-928.

Bonini, M., Corti, G., Innocenti, F., Manetti, P., Mazzarini, F., Abebe, T. and Pecskay, Z.., 2005. Evolution of the Main Ethiopian Rift in the frame of Afar and Kenya rifts propagation. *Tectonics,* 24, TC1007. DOI: 10.1029/ 2004TC001680.

Cantwell, T., Detection and analysis of low frequency magnetotelluric signals, *Ph.D. thesis, Geology and Geophysics, M.I.T.,* 170 pp., 1960.

Ebinger, C.J. and Casey, M., 2001: Continental breakup in magmatic provinces, an Ethiopian example. *Geology* 29, 527–530.

Eysteinsson, H., 1998: TEMMAP and TEMCROSS plotting programs. *ÍSOR – Iceland GeoSurvey*, Unpublished programs and manuals.

Flóvenz, Ó.G., Hersir, G.P., Saemundsson, K., Ármannsson, H., and Fridriksson Th., 2012: Geothermal energy exploration techniques. *In: Sayigh, A. (ed.), Comprehensive renewable energy, vol 7*. Elsevier Oxford, United Kingdom, 51-95.

Flóvenz, Ó.G., Spangerberg, E., Kulenkampff, J., Árnason, K., Karlsdóttir, R., Huenges, E., 2005: The role of electrical interface conduction in geothermal exploration. *Proceeding of the World Geothermal Congress 2005*, Antalya, Turkey, 9 pp.

Gebrewold,Y., 2017: Geothermal Geochemistry of Butajira prospect area, Central Main Ethiopian implication for potential areas to geothermal energy in Ethiopia. *Geological survey of Ethiopia (GSE),* unpublished report.

Hersir, G.P., and Árnason K., 2009: Resistivity of rocks. *Paper presented at "Short Course on Surface Exploration for Geothermal Resources", organized by UNU-GTP and LaGeo, Santa Tecla, El Salvador, UNU-GTP SC-09*, 8 pp.

Kebede, S., 2014: Geothermal exploration and development in Ethiopia: country update report, presented short course IX on exploration for geothermal resource 2014, , *organized by UNU-GTP, KenGen and GDC, Naivasha, Kenya*, UNU-GTP 22 pp.

Keller, G.V., and Frischknecht, F.C., 1966: Electrical methods in geophysical prospecting. *Pergamon Press*, NY, 527 pp.

Lahitte, P., Gillot, P.Y., Courtillot, V., 2003: Silicic central volcanoes as precursors to rift propagation: the Afar case. *Earth Planet. Sci. Lett.* 207, 103–116.

Lemma, Y., 2010: Multidimensional Inversion of MT data from Krýsuvík High Temperature Geothermal Field, SW-Iceland, and study how 1D and 2D inversion can re-produce a given 2D/3D resistivity structure using synthetic MT data. University of Iceland, Faculty of Earth Sciences, MSc thesis, UNU-GTP, report 4, 94 pp. of Iceland, *MSc thesis*, *UNU-GTP,* report 1, 92 pp.

Le Turdu, C., Tiercelin, J.J., Gibert, E., Travi, Y., Lezzar, K.E., Richert, J.P., Massault, M., Gasse, F., Bonnefille, R., Decobert, M., Gensous, B., Jeudy, V., Tamrat, E., Mohammed, M.U., Martens, K., Atnafu, B., Cherent, T., Williamson, D., Taieb, M., 1999: The Ziway-Shala lake basin system, Main Ethiopian Rift: influence of volcanism, tectonics and climatic forcing on basin formation and sedimentation. *Palaeogeogr. Palaeoclimatol. Palaeoecol.* 150, 135–177.

Mohr, P.A., 1962: The Ethiopian Rift System. *Bull. Geopys. Obs. Addis Ababa University* 5, 33–62.

Phoenix Geophysics, 2005: Data processing. User guides. Phoenix Geophysics, Ltd., Toronto. Press Ltd., Oxford, 527 pp.

Pik, R., Deniel, C., Coulon, G., Hofmann, C., Ayalew, D., 1998: The North Western Ethiopia Plateau Flood Basalts. Classification and spatial distribution of magma types. *J. Volcanol., Geotherm, Res,* 81, 91-111.

Pizzi, A., Coltorti, M., Abebe, B., Disperati, L., Sacchi, G., & Salvini, R., 2006: Wonji fault belt (Main Ethiopian Rift): structural and geomorphological constraints and GPS monitoring. The Afar Volcanic Province within the East African Rift System. *Geological Society, London, Special Publications*, 259, 191–207.

Tikhonov, A.N., 1986: On determining electrical characteristics of the deep layers of the Earth's crust. *Dokl. Akad. Nauk.* USSR, 73, 295-297.

Ukstins, I.A., Renne, P.R., Wolfenden, E., Baker, J., Ayalew, D., Menzies, M., 2002: Matching conjugate rifted margins 40 Ar/39 Ar Chrono – Stratigraphy of pre and syn-reft bimodal flood volcanism in Ethiopia and Yemen. *Earth and Planetary Science Letters* 198, 289-306.

UNDP, 1973: Geology, geochemistry and hydrology of hot springs of the East African Rift System within Ethiopia. *UNDP, December report* DD/SF/ON/11, NY.

Vozoff, K., 1972: The magnetotelluric method in the exploration of sedimentary basins: *Geophysics, v.* 37, p. 980–1041.